

Supporting Information

A Full Solar Light Spectrum Responsive B@ZrO₂-OV Photocatalyst: A Synergistic Strategy for Visible-to-NIR Photon Harvesting

Yumei Qin,^{‡ a} Zhaoyang Ding,^{‡ a} Wenwei Guo,^a Xiaolu Guo,^a Cheng Hou,^a Bang-Ping Jiang,^a Chun-Guang Liu,^b Xing-Can Shen^{ a}*

^a Key Laboratory for the Chemistry and Molecular Engineering of Medicinal Resources, School of Chemistry and Pharmaceutical Science, Guangxi Normal University, 15 Yucai Road, Guilin, 541004, P. R. China

^b Department of Chemistry, Beihua University, 15 Jilin Street, Jilin, 132013, P. R. China

[‡]These authors contributed equally to this work

*E-mail: xcshen@mailbox.gxnu.edu.cn

Number of Pages: 6

Number of Figures: 10

Number of Tables: 3

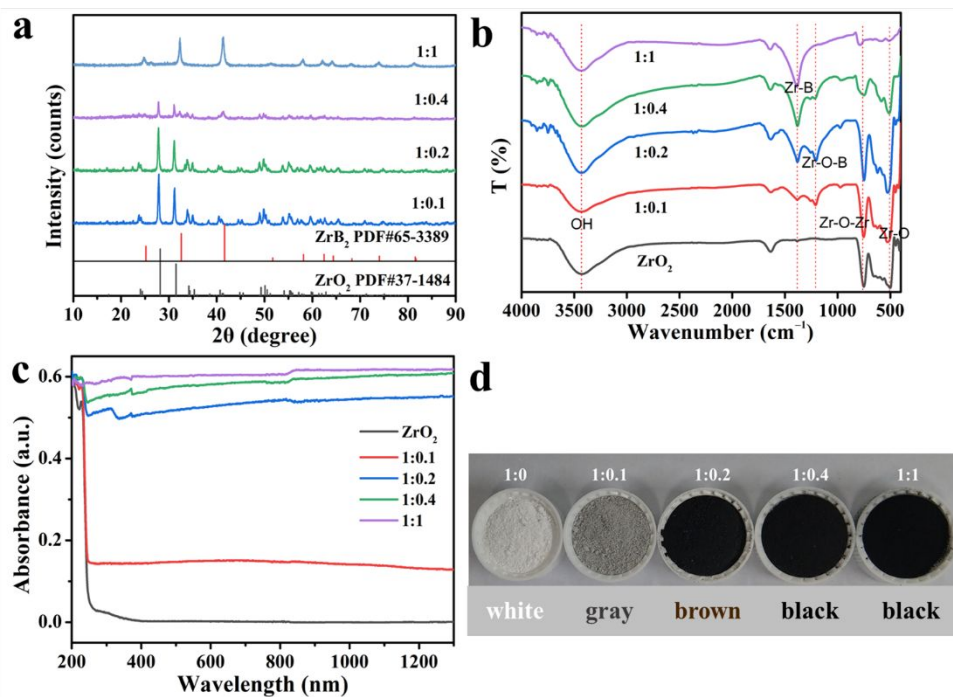


Figure S1. (a) XRD patterns, (b) FT-IR spectra, (c) UV-vis-NIR diffuse reflectance spectra and (d) photographs of ZrO_2 reacted with different amount of $NaBH_4$.

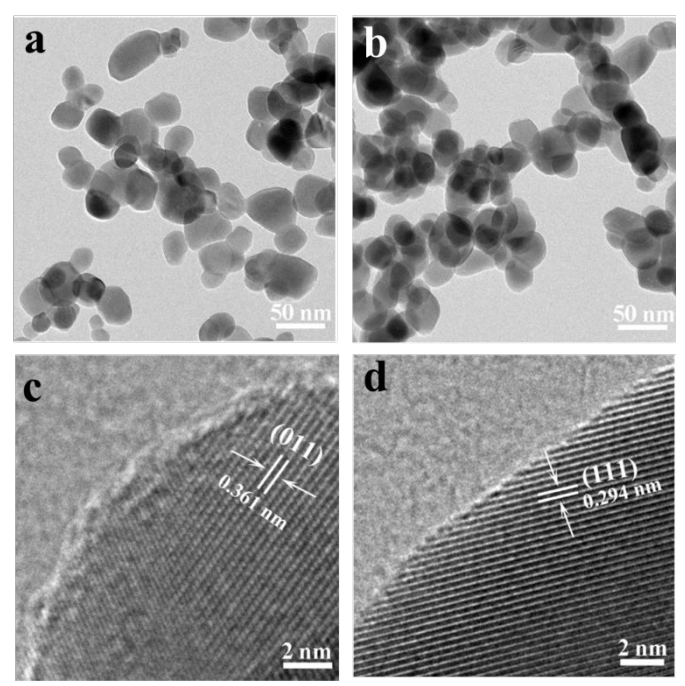


Figure S2. TEM image of (a) ZrO_2 -OV, and (b) ZrO_2 and HRTEM image of (c) ZrO_2 -OV, and (d) ZrO_2 .

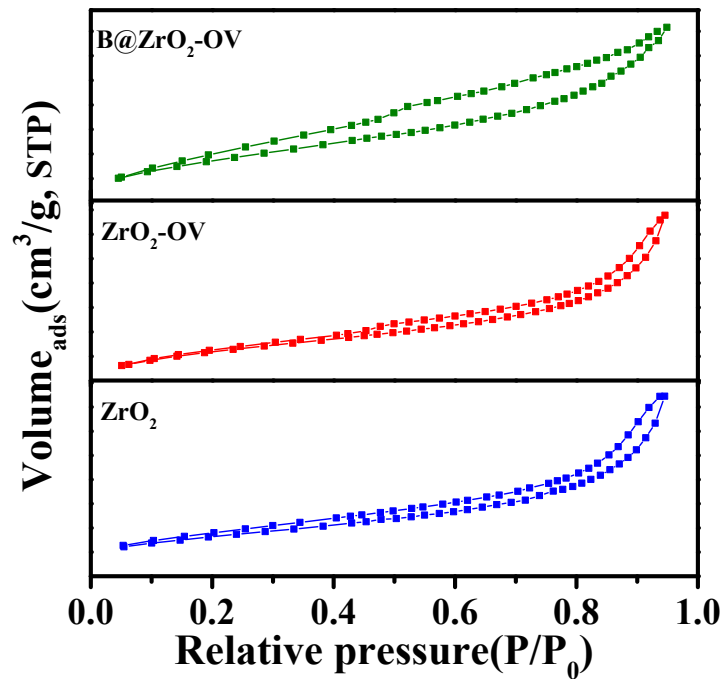


Figure S3. N₂ adsorption-desorption isotherm of ZrO₂, ZrO₂-OV and B@ZrO₂-OV.

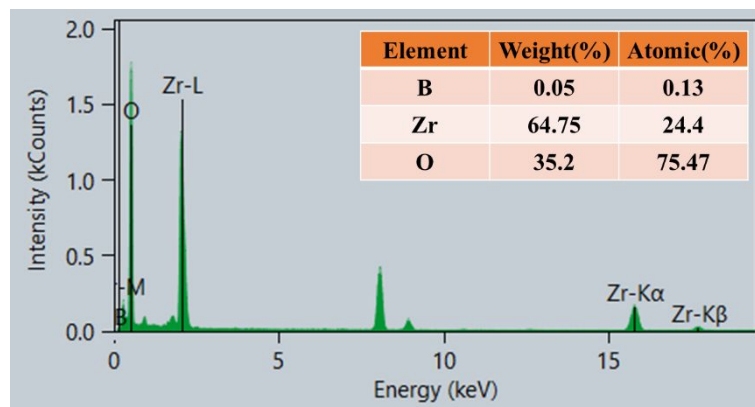


Figure S4. EDS quantitative analysis of B@ZrO₂-OV. Inset: The element content of B, O and Zr.

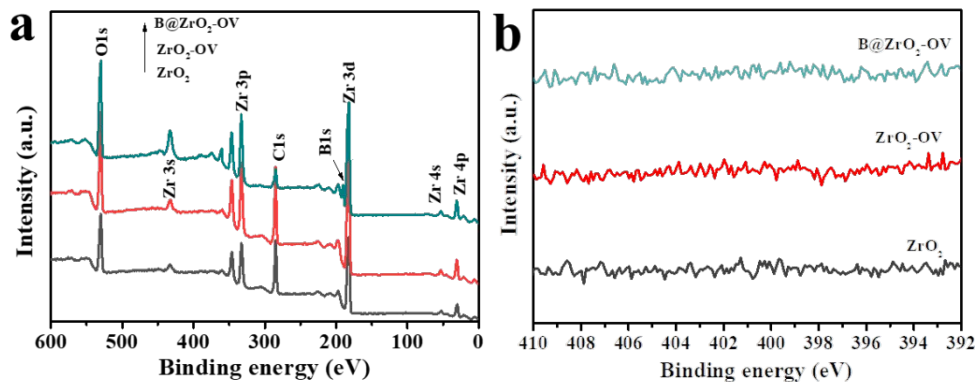


Figure S5. (a) Full XPS survey spectra and (b) high-resolution XPS for N 1s of the ZrO₂, ZrO₂-OV and B@ZrO₂-OV.

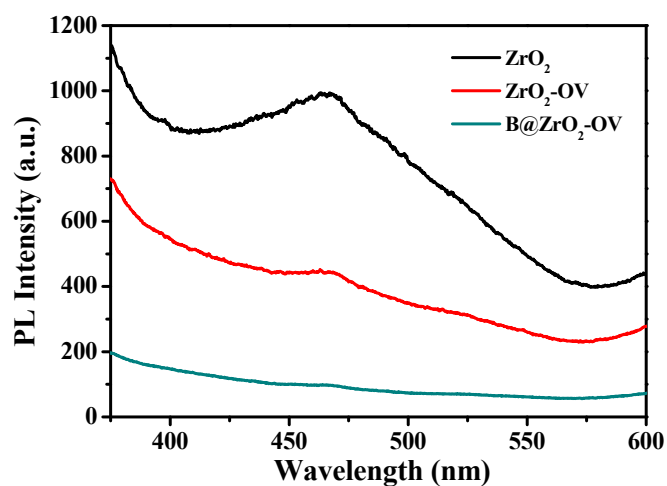


Figure S6. PL spectra of the ZrO_2 , $\text{ZrO}_2\text{-OV}$ and $\text{B@ZrO}_2\text{-OV}$.

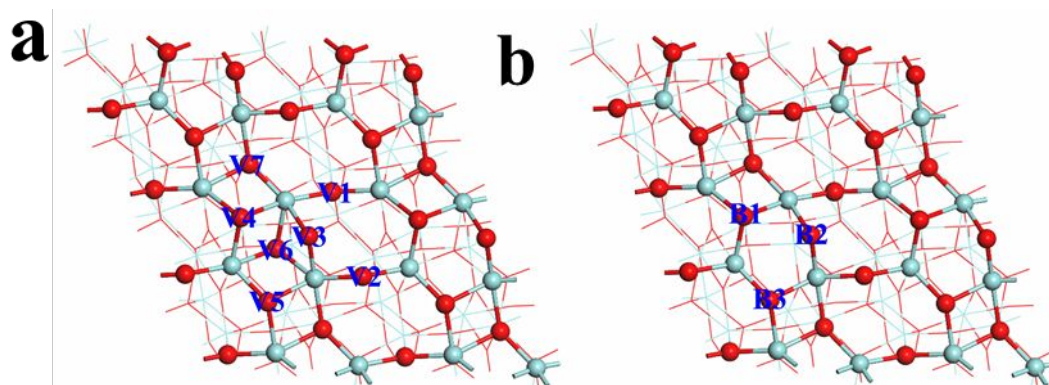


Figure S7. Different oxygen vacancy sites on the surface of ZrO_2 (a) and different B sites on the $\text{ZrO}_2\text{-OV}$ (b). Zr, O, B atoms and oxygen vacancy are represented as cyan, red, and green color.

Table S1. The formation energy of oxygen vacancy (OV) with different oxygen vacancy sites

Structure	V1	V2	V3	V4	V5	V6	V7
E_f	6.21	6.57	6.34	6.14	6.30	5.52	5.79

Table S2. The formation energy of oxygen vacancy (OV) with different B sites

Structure	B1	B2	B3
E_f	4.848	4.849	6.137

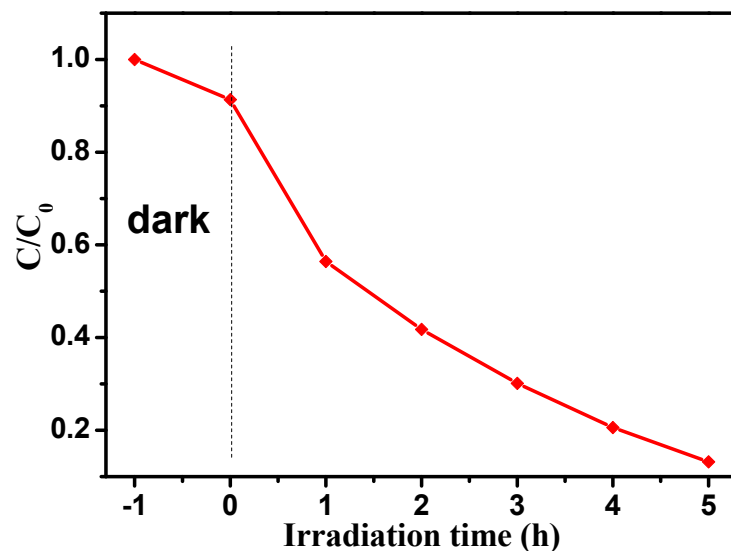


Figure S8. Photocatalytic degradation of RhB by B@ZrO₂-OV catalyst under simulated solar light irradiation.

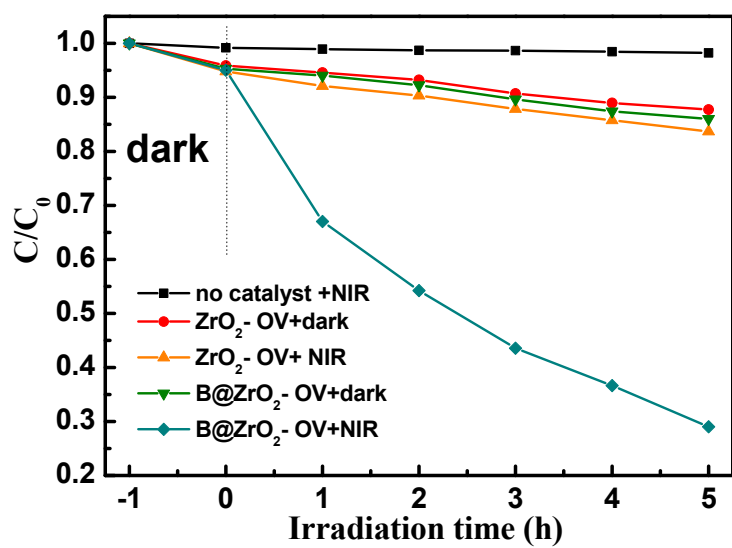


Figure S9. Photocatalytic degradation of phenol over B@ZrO₂-OV and ZrO₂-OV in the absence and presence of NIR light irradiation.

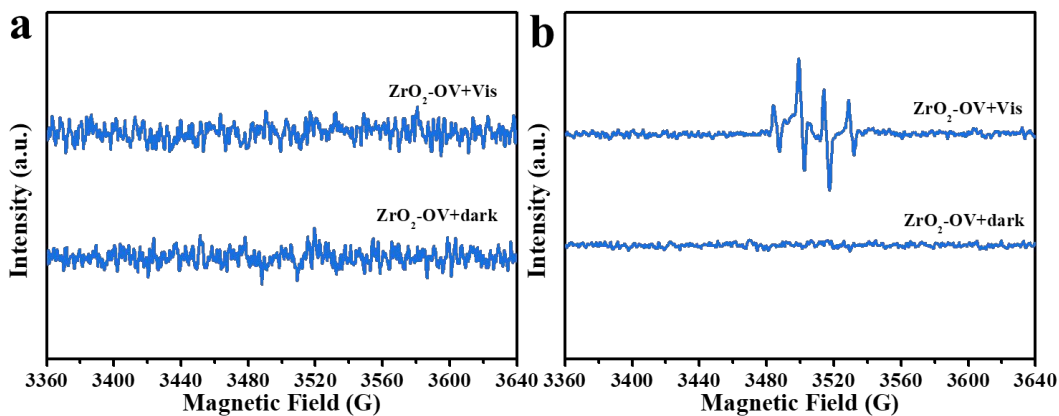


Figure S10. EPR signals of the (a) DMPO- $\cdot\text{O}_2^-$ and (b) DMPO- $\cdot\text{OH}$ for 5 min under visible light irradiation with the presence of $\text{ZrO}_2\text{-OV}$.

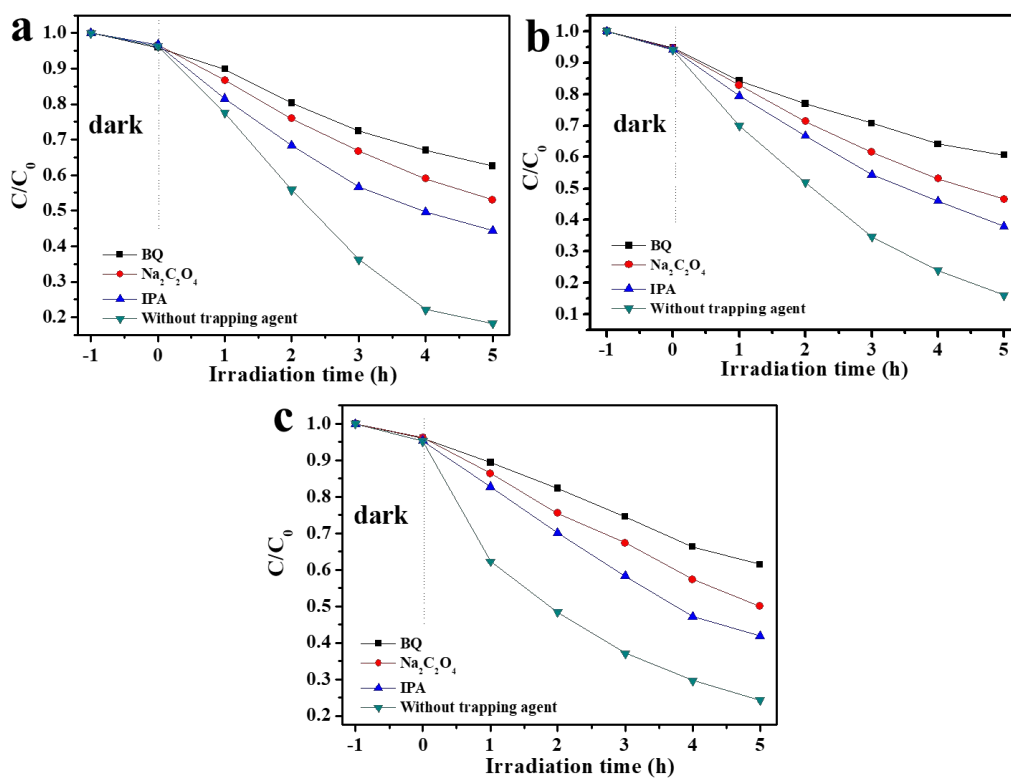


Figure S11. Effects of different reactive species scavengers on the photodegradation of RhB by $\text{B@ZrO}_2\text{-OV}$ under NIR (a), visible (b) and UV (c) light irradiation.

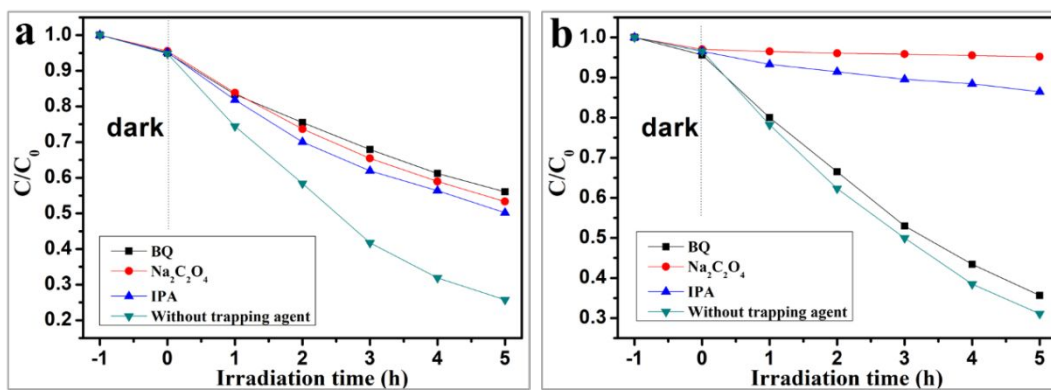


Figure S12. Effects of different reactive species scavengers on the photodegradation of RhB by $\text{ZrO}_2\text{-OV}$ under UV (a) and visible light (b) irradiation.